Aalborg Universitet

Dynamic Stabilization of DC Microgrids Using ANN-Based Model Predictive Control

Akpolat, Alper Nabi; Habibi, Mohammad Reza; Baghaee, Hamid Reza; Dursun, Erkan; Kuzucuoglu, Ahmet Emin; Yang, Yongheng; Dragicevic, Tomislav; Blaabjerg, Frede

Dynamic Stabilization of DC Microgrids using ANN-Based Model Predictive Control

Alper Nabi Akpolat, *Member, IEEE*, Mohammad Reza Habibi, *Student Member, IEEE*,
Hamid Reza Baghaee, *Member*, *IEEE*, Erkan Dursun, *Member, IEEE,* Ahmet Emin Kuzucuoğlu, *Member, IEEE,*
Yongheng Yang, *Senior Member, IEEE,* Tomislav Dragičević, *Senior Member, IEEE,* Frede Blaabjerg, *Fellow, IEEE*

Abstract—**Over the past decade, the high penetration of renewable-based distributed generation (DG) units has witnessed a considerable rise in electrical networks. In this context, direct current (DC) microgrids based on DGs are being preferred due to having less complexity for the establishment and control. At the same time, they offer higher efficiency and reliability compared to their alternating current (AC) counterparts. This paper proposes a new model predictive control (MPC)-trained artificial neural network (ANN) control strategy being an ANN-MPC instead of conventional cascaded-proportional-integral (PI)-trained ANN control for dynamic damping of photovoltaic (PV)-battery-based grid-connected DC microgrids. Unlike traditional controllers, the proposed control approach more rapidly attains generation-load power balancing under variable climate input (meteorological sensor data) and output (load demand), hence achieving quick DC-bus voltage damping. The proposed ANN-MPC scheme is examined under different operating conditions, and the results are compared with the ANN-based conventional PI controller. The results show the proposed control strategy's efficacy to lessen the instability issues and achieve effective attenuation of oscillations in DC microgrids.**

Index Terms—**Artificial neural network (ANN), battery energy storage system (BESS), DC microgrids, model predictive controller (MPC), photovoltaics (PVs).**

I. INTRODUCTION

BECAUSE of technical, environmental, and economic reasons, an increasing interest is shown by the energy sector in adopting micro and smart grid technologies to enhance future electricity grids' efficiency and reliability [1]. A microgrid is a small-scale power grid that can solve energy issues and enhance the flexibility locally and operate either in a grid-connected or autonomous operation mode. Compared with the alternating current (AC) microgrids, direct current (DC) microgrids have the advantages of higher efficiency, lower implementation cost, simpler control, and higher reliability [2]. Moreover, reactive power flows, voltage unbalances, and harmonics are absent

A. N. Akpolat, E. Dursun, and A. E. Kuzucuoğlu are with the Department of Electrical-Electronics Engineering, Faculty of Technology, Marmara University, Istanbul, 34854, Turkey (e-mails: alper.nabi@marmara.edu.tr, erkandursun@marmara.edu.tr, and kuzucuoglu@marmara.edu.tr). M.R. Habibi and F. Blaabjerg are with the Department of Energy Technology, Aalborg University, Aalborg East, 9220, Denmark (e-mails: mre@et.aau.dk and fbl@et.aau.dk). H.R. Baghaee is with the Department of Electrical Engineering, Amirkabir University of Technology, Tehran, 15914, Iran (e-mail: hrbaghaee@aut.ac.ir). Y. Yang is with the College of Electrical Engineering, Zhejiang University, Hangzhou 310027, China (email: yang_yh@zju.edu.cn). T. Dragičević is with the Department of Electrical Engineering, Center of Electric Power and Energy, Technical University of Denmark, 2800 Kongens Lyngby, Denmark (e-mail: tomdr@elektro.dtu.dk).

from the DC microgrid, makes it easier to control [3]. With the continuous advancement of control theory, many advanced control algorithms [4] have been developed recently. In this context, researchers have proposed various control frameworks such as centralized control [5], distributed control [6], and hierarchical control [7], to meet the communication requirements in practical projects to ensure normal operations of the microgrids. Among advanced control methods, model predictive control is seen as one of the most versatile advanced control methods for DC microgrids [3]. Model predictive control (MPC)-based strategies have been proposed for control of hybrid AC/DC [1], [8], [9], AC [10], [11], and DC microgrids, [12]–[19], [20]. In AC and hybrid AC/DC microgrids, the MPC-based strategies have been proposed for the control of AC/DC [8], [9], and DC/DC bidirectional interlinking converters (BICs) [1]. In DC microgrids, different MPC-based techniques have been proposed for stability improvement [15], [16] optimal energy management [3], improving power-sharing [4], control of DC microgrids including constant power loads (CPLs) [12], [17], [18], high-performance control of DC microgrid with a good transient tracking error [21], control of naval DC microgrids supplying pulsed power loads [13], [14], mitigating distribution power loss of DC microgrids with DC electric springs [22], control of DC/DC BICs [1], [20], and maximum power point tracking of photovoltaic (PV) sources [19]. As known, MPCs possess some features such as the basic inclusion of systems constraints and nonlinearities, flexibility to implement, and time-consuming behavior due to progressing optimization and prediction processes to manage the plant [23]. Thus, that behavior results in a computational burden issue unexpectedly. The weighting factor have been determined in the cost function of the MPC through artificial neural networks (ANNs) [24] for obtaining robustness with a novel method. To reduce the computational burden of MPCs for controlling modular multilevel converters, a neural network (NN) regression controller is introduced [25]. As ANN-based techniques do not need any information or mathematical model of the system in which it is implemented and also do not have a heavy computational burden, it is noteworthy to perform.

Similarly, some approaches have been reported to further improve the control techniques. Therefore, the application of smart methodologies has been becoming prominent in the control area of DC microgrids [26]. In particular, ANN-based controllers have been broadly utilized for problem identification [27], voltage sag classifications [28], short-term prediction [29], etc., which is a subset of artificial intelligence

(AI) and also machine learning (ML) technology. Some examples are regulating the DC-bus voltage of a hybrid AC/DC microgrid through feedforward NNs with low computational burden [30], obtaining robustness in dual active bridge structure for DC microgrids [31] with ANN-based proportional-integral (PI) controllers in terms of over-undershoot, rise-fall time, and settling time, etc., and mitigating the steady-state oscillations with the help of ANN-based PI sensorless controllers [32] and ANFIS-power oscillation damping controllers [33] that contain the benefits of the ANNs and the fuzzy logic. Due to these benefits, more complex ANN structures, e.g., deep supervised learning-based ANN architecture have been proposed to capture the system dynamics with high accuracy rates in the control of the DC/DC converter [34] and also actor-critic ANN architecture regulates the voltage of the DC bus with current sharing at the same time [35]. Furthermore, the ANNs are implemented in this field such as the control of a DC/DC converter to maintain stable output voltage [36] and also in the AC microgrid applications, e.g., sensorless voltage prediction method for total harmonic distortion (THD) calculation is presented [37].

This paper aims to bridge these disadvantages, such as computational burden, steady-state oscillations, slowness, and others. To this end, a new control strategy is proposed by combining the MPC and ANNs, which are trained through the robust behavior of the MPC to tackle the drawbacks of the mentioned controllers. In other words, the proposed method is implemented by replacing MPC with ANNs instead of merely applying MPC to alleviate the disadvantages in DC microgrids, including PV units and battery energy storage systems (BESSs). Similarly, one of the biggest motivations of this study is to provide more effective stabilization in DC-bus parameters by improving the results obtained as a result of the training of the ANNs to be trained with different controllers. Using the MPC's robust stability features can rapidly provide robust behavior and desired training datasets under load changes and variable input and output conditions, dissimilar to the reported PI-based control schemes. The theoretical concepts and basic modeling of the DC microgrid system are provided, and the training procedure of ANN for realizing the ANN-based MPC scheme is explained. Briefly, the main features of proposed method can be summarized as follows:

1) Using the MPC's robust stability features rapidly provides robust behavior and more proper training datasets under load changes and variable input and output conditions, dissimilar to the utilized PI-based control schemes.

2) Additionally, the ANN-based MPC control scheme has the merits of flexible and enhanced system robustness by achieving more effective attenuation in the steady-state, superior to ANN-based PI.

3) The obtained simulation results and comparisons can conclusively prove the effectiveness, accuracy, and authenticity of the proposed method for the dynamic stabilization of DC microgrids.

Finally, to prove the effectiveness of the proposed ANN-based MPC strategy, offline digital time-domain simulation studies are performed on a test DC microgrid system in MATLAB/Simulink environment, and all obtained results are compared with each other. For the sake of obtaining more
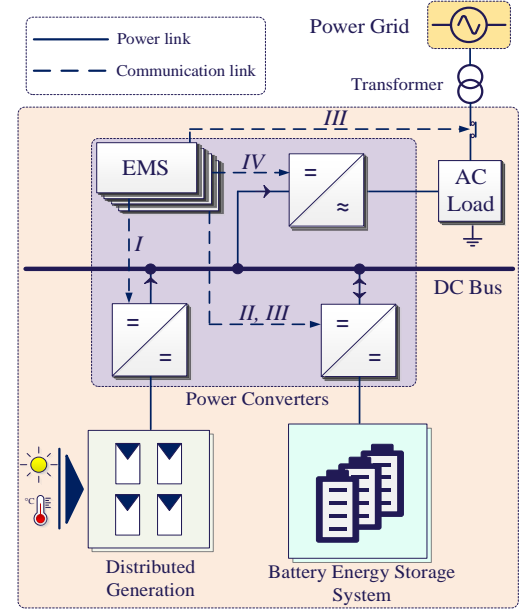

Fig. 1. Overview of proposed PV- Battery based DC microgrid.

TABLE I
PARAMETERS OF ENERGY CONVERSION SYSTEM COMPONENTS

DG: PV ARRAY	
Rated Maximum Power-P_m (kW)	1
Maximum Power Current-I_{mp} (A)	32.68
Maximum Power Voltage-V_{mp} (V)	30.6
Short Circuit Current-I_{sc} (A)	34.83
Open Circuit Voltage-V_{oc} (V)	36.3
Module Efficiency-η (%)	15.40

BATTERY ENERGY STORAGE SYSTEM (BESS)	
Battery Type	Lead-Acid
Nominal Voltage (V)	12
Nominal Capacity (Ah)	200
Internal Resistance (mΩ)	3.4
Cut-off Voltage (V)	9
Fully Charge Voltage (V)	13.6

realistic results, the input dataset of distributed generation (DG) is supplied with the help of a weather station, and the real-time experimental setup of the PV side (i.e., DG) and the BESS are performed by measuring their dynamics and then embedded in the simulation. The performance of the proposed strategy is evaluated in different operating conditions.

To cover the mentioned themes, the rest of this paper is organized as follows: Section II elaborates on the physical structure of the DC microgrid and its conventional cascaded-PI-based control scheme. The proposed ANN-based MPC strategy is presented in Section III. Offline digital time-domain simulation studies and comparisons are provided in Section IV. Finally, discussions and conclusions are stated in Sections V and VI, respectively.

II. OVERVIEW OF CONVENTIONAL DC MICROGRID ARCHITECTURE

A. Physical Structure of DC Microgrid

Fig. 1 depicts the overview of conventional DC microgrid architecture under study. The system comprises a PV array, a BESS, power converters, load, and grid parts. As to a DG, the PV array is linked to a DC bus with its unidirectional DC/DC converter. The BESS is also connected to the same DC bus
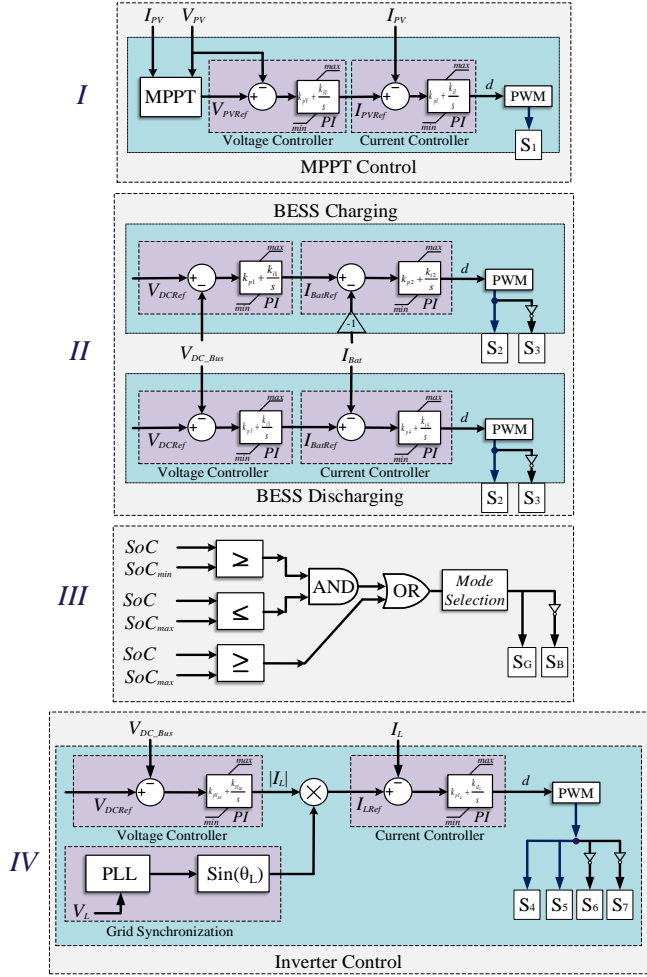
Fig. 2. Conventional control strategy with cascaded-PI for DC microgrid.

through a bidirectional DC/DC bus converter. Variable AC loads have been included in the system. The AC bus is tied to the DC bus with an AC/DC BIC. The model represents a real platform to some extent. Regarding connections among the elements, solid lines possess power, whereas intermittent ones belong to the communication line. The above-mentioned DC microgrid ensures to feed the AC loads interruptedly with a DC/AC inverter operation. The power grid is connected to the DC microgrid from the transformer. An energy management system (EMS) controls the power converters coordinately to provide power flow smoothly. In this microgrid, the total rating power of the PV array is 1 kW. Also, the PV side has a maximum power point tracking (MPPT). We have tried to maximize battery capacity as much as the physical and financial situations allow while establishing the system. In order to provide longer sustainable energy to the load side once the PV input has a lack of power generation, we have selected six pieces of batteries, three pieces connected in parallel and two pieces of them in series. Each of them has a 200 Ah capacity with nominal 12 V output voltage. Thereby, the BESS's capacity corresponds 600 Ah, and its nominal output voltage reaches 24 V, with 14.4 kWh energy capacity. The parameters of the system components are given in Table I. The BESS plays a vital role in improving the microgrid's stability and alleviating the effects of the variable nature of the RESs. The primary power source to the loads is the PV array; however, the BESS

stores surplus power generated from the PV side as complementary power sources. This operation form makes the system more stable and robust.

B. Traditional Control Scheme for General System

To determine the system's behavior under different control schemes in this paper, we first implemented cascaded-PI reference voltage-current control, then controlled through MPC, and lastly performed the trained ANNs with the help of the cascaded-PI and MPC separately. The data were obtained and compared using these controllers. As known, any controller is one of the systems' main parts for achieving a high-performance. Fig. 2 shows the general scheme of the implemented cascaded-PI reference voltage-current control. The system contains eight switches controlled for uninterrupted power flow from DG to loads or grid to loads. The first (I) controller belongs to the PV converter by its MPPT controller. Solar cells from the PV systems are nonlinear characteristics and are considered to operate the maximum power point (MPP) under those changes [38]. The most forceful method for better harvesting energy from PV cells is the MPPT technique. A bidirectional DC/DC buck-boost BESS converter is one of the key elements for managing the deficit or surplus powers among DGs, loads, and power grid through the second (II) and third (III) controllers. The third one also enables us to keep the BESS working in a predefined state of charge (SoC) band. The SoC value can be calculated with the ampere-hour (coulomb) counting method. This method assumes that the battery capacity is known, and battery parameters like voltage and current can be measured accurately. On the other hand, a full cycle is defined as complete discharge, and charges to 100% depth of discharge (DoD) value is described as follows

$$SoC = 1 - DoD. \tag{1}$$

If the SoC is 100% or equal to 1, it represents a fully charged battery, and 0% is for an empty battery. SoC_i is the initial value of the SoC, which is calculated as

$$SoC = SoC_i - \frac{1}{Q}\int_{t_2}^{t_1} i_{Batt} dt. \tag{2}$$

The mentioned system has two different operation modes versus the demand regarding battery and grid mode. In the battery mode, the batteries are fed by the DG, and subsequently the loads are also fed. Despite the fact that BESS is discharged up to a certain SoC_{min} level, the inverter dispatches the power from the BESS to the loads in the battery mode. On the contrary, in the grid mode, unless the SoC level is higher than the minimum value, i.e., SoC_{min}, the BESS needs to be charged and charged by the utility grid. The BESS control strategy can be divided into two different stages as the step-down and step-up stages correspond to switches in the unidirectional DC/DC buck-boost converter responsible for charging and discharging, respectively. The step-up stage is controlled and the step-down one is closed while discharging exists. On the contrary, step-down one is active while charging exists. Both charging and discharging control modes have DC-bus voltage and current references for the outer and inner loops. If the DC-bus voltage is higher than the defined reference, the inner current loop tunes the duty cycle to force the current flow from the DC-bus to the BESS, which introduces charging the BESS. The batteries'

utilization and lifetime should be paid attention to due to their total cost of ownership. So, the batteries should be operated at a defined *SoC* level by

$$SoC_{\min} \le SoC \le SoC_{\max}. \tag{3}$$

Besides, the BESS is expected to dispatch power to the load side in the battery mode as well, once the *SoC* value is higher than *SoC_{max}*. In other words, if the desired *SoC* value is less than *SoC_{min}*, the system should switch on the grid-tied mode; otherwise, it should keep working in battery (standalone) mode. On the other hand, confining an *SoC* band provide a healthy operation eliminating overcharge and disruptive discharge [39]. In the grid mode, the EMS is also can send the commads to charge-discharge the BESSas a tertiary control with the help of static S_G switch. Thereby, the EMS changes the static switch's state (S_G) to transfer power from the grid to the load side while energy harvesting and *SoC* are less than demand; vice versa i.e., battery mode is switched on by another static switch (S_B). As can be seen in Fig. 2, control loops and EMS affect semiconductor devices' switches that can be classified as follows: S_1 exits in the DC/DC boost converter, S_2-S_3 couple belongs to the unidirectional DC/DC buck-boost converter, and lastly, the rest of switches are located in the unidirectional DC/AC inverter.

Additionally, the BESS converters can also regulate the battery banks charging rates in grid mode. Based on the *SoC* values and the demand conditions on the load side, the charging-discharging current references are generated to regulate the current flow in the converters. To this end, the BESS can inject power to the DC bus or absorb power from the DC bus. In this case, only one current control close loop with a PI controller is enough to regulate the charging current. Lastly, the fourth (*IV*) one exists for inverter control, depending on the system mode. Each control layer affects each other indirectly to operate synchronously.

III. ARTIFICIAL NEURAL NETWORK-BASED MODEL PREDICTIVE CONTROL

A. Model Predictive Control of DC Microgrid

MPC is using in different power applications, e.g., control of power converters in AC microgrids [40], dynamic stabilization for a DC microgrid [16], and introduced a schedule approach for the operation of domestic refrigerators [41]. Model predictive-based controllers can have advantages compared to conventional controllers, but MPC has the main drawback, making it hard to implement in the system. The MPC's main disadvantage is the time-consuming behavior due to using optimization and prediction approaches to control the system. MPC needs to predict the future and do optimization to find proper values for the manipulated variables. Therefore, it will do a process with a heavy computational burden, which can be time-consuming. In this paper, to cover MPC's drawbacks, ANNs are used. The ANNs are trained based on MPC-based data to behave as the implemented model predictive-based controller to overcome MPC's problem, i.e., time-consuming control application. The model predictive control-based approach attempts to predict the plant output's future values and uses this in an optimization process to find the proper plant

inputs. If the state in the system is as follows:

$$\begin{cases} x(k+1) = Ax(k) + Bu(k) \\ y(k) = Cx(k) \end{cases}, \tag{4}$$

the future values of the plan outputs can be calculated as follows [42], [43]:

$$Y = Ex(k) + Gu(k-1) + L\Delta U, \tag{5}$$

where,

$$Y = \begin{bmatrix} y(k+1) \\ y(k+2) \\ \vdots \\ y(k+P) \end{bmatrix}, \tag{6}$$

$$\Delta U = \begin{bmatrix} \Delta u(k) \\ \vdots \\ \Delta u(k+P-1) \end{bmatrix}, \tag{7}$$

$$E^T = \begin{bmatrix} CA & CA^2 & \cdots & CA^P \end{bmatrix}, \tag{8}$$

$$G^T = \begin{bmatrix} CB & \cdots & \sum_{q=0}^{P-1} CA^q B \end{bmatrix}, \tag{9}$$

$$L = \begin{bmatrix} CB & 0 & \cdots & 0 \\ CAB + CB & CB & \cdots & 0 \\ \vdots & \vdots & \vdots & \vdots \\ \sum_{q=0}^{P-1} CA^q B & \sum_{q=0}^{P-2} CA^q B & \cdots & CB \end{bmatrix}. \tag{10}$$

In (4), *x*, *u*, and *y* represent the plant's state, manipulated variables, the plant's input, and the plant output. *u(k)* is the manipulated variable as long as assuming the input is generated by a sample and hold the device as *u(t)=u(k)*, $kh \le t \le (k+1)h$. With respect to, $t_0= kh$ and $t=(k+1)h$, it can be expressed *x(kh)=x(k)*, namely, *u(k)* is constant on the interval [*kh*,(*k*+1)*h*]. As seen in (7), ΔU is our control objective is to form a control sequence as $\Delta U(k)$, $\Delta U(k+1)$, …, $\Delta U(k+P-1)$, where *P* is the prediction horizon. It is important to note that MPC uses a cost function to obtain the plant input's proper values, and the plant's prediction values can be used to make the cost function. The cost function can be defined as:

$$I(W_k) = \sum_{i=1}^{P} \left(\alpha_i \left(r(k+i \mid k) - y(k+i \mid k) \right) \right)^2 + \lambda \theta_k^2, \tag{11}$$

where,

$$W_k^T = [u(k \mid k)^T \quad \cdots \quad u(k+P-1 \mid k)^T \quad \theta_k]. \tag{12}$$

In (11) and (12), α_i, *r*, λ, and θ_k are the weighting coefficient reflecting the relaive importance of the controlled variable, reference the output, weight of the constraint violation penalty, and slack variable respectively. In this paper, four models of the predictive-based controller are implemented. The first couple is used to control the DC/DC power converter of the PV system. The third MPC is implemented to control the BESS's bidirectional DC/DC power converter. The fourth controller is used to control the AC load. Also, the plant input, plant output,

and the reference for the four mentioned MPCs are defined as follows:

a) For the first MPC, the plant predicts reference current through V_{PV} and its reference V_{REF}, instead of the PI voltage controller.

b) Similarly, the second plant utilizes I_{PV} and I_{REF} for controlling the DC/DC boost PV converter as desired.

c) For controlling the DC/DC buck-boost BESS converter, another model predictive plant is developed by obtaining V_{DC_Bus} and its reference V_{REF_Bus}.

d) The last predictive plant is deployed for operating the DC/AC interlinking inverter to dispatch the power from the DC bus to the AC loads with the help of measurements of V_{DC_Bus}, V_{Load}, and I_{Load} signals.

After compiling a normal operation to gather training data for ANNs, the system becomes ready for the exploitation phase with trained ANNs.

B. Implementation of ANN

Typically, an ANN is considered a subset of artificial intelligence (AI) that tries to imitate the human brain's mindset. Dynamic ANNs contain tapped delay lines that are ready for nonlinear prediction. They are also appropriate for impending failure detection, regression problems, system identifications, and dynamic modeling of a physical model [37]. This study presents a multi-layer feedforward NN with Levenberg-Marquardt backpropagation structure, which is a pretty simple structure among NNs and easy to apply, as can be seen in Fig. 3. Thereby, with the aim of avoiding unnecessary complexity, we have targeted to apply one of the essential feedforward NNs to conduct simplicity. The reason why this ANN structure is adopted is that it does not make the system complex for solving the regression estimate problem which is faced. In particular, the elements of the feedforward ANNs are divided by layers. The signs from the input layer to the output are carried by a one-way connection. While linking one layer to the next, any link does not exist in the same layer. In feedforward networks, the outputs of the cells in the layers are the input of the next layer. If the layer by layer network is examined, the input layer carries the information from theexternal environment to the cells in the intermediate (hidden) layer without making any changes. The output of the network is calculated by processing it in the hidden layers and the output layer. For the input presented to the network, the output of the network is compared with the genuine result. The difference arising from this comparison reveals the error value. The purpose of calculating backpropagation is to generate a decent output by reducing the error [37]. The error will be distributed to the weight ratings of the network every iteration. The mentioned feedforward networks usually meet problems such as regression, classification, and prediction by preferring the delta supervised learning rule that is predefined with the help of the known output dataset.

Since nonlinear problems cannot be learned with single-layer perception, most of the problems encountered in daily life are linear. In other words, the feedforward network can imitate static nonlinear relationships dissimilar to recurrent networks that are used for dynamic relationships. As static relationships are necessary, the feedforward NNs would be convenient.
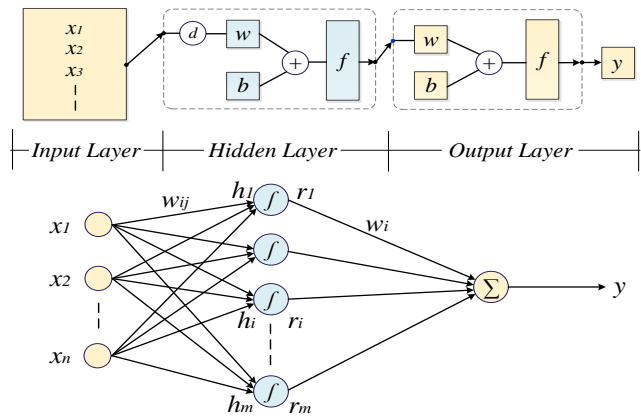

Fig. 3. Schematic structure of ANN to estimate output (W: weights, b: bias, and f: activation function) [44].

Referring to the operation, an ANN predicts data series of $y(t)$ while obtaining past values up to delay (d) pieces of x(t) series as

$$y(t) = f\left(x(t-1),...,x(t-d)\right). \qquad (13)$$

The NN can be designed under four sections such as proper input selection, defining the paradigms, estimation, and lastly implementation. The backpropagation is a methodology to train the weights in a multi-layer feedforward NN [44]. If the network has n inputs, one hidden layer with m neurons, and one output, the generic structure of the backpropagation NN can be stated as follows:

$$b_k = \left\{b_{k,j} \,|\, 1 \le j \le m\right\}, \qquad (14)$$

$$w_t = \left\{w_{t,ij} \,|\, 1 \le i \le n \ \ and \ \ 1 \le j \le m\right\}, \qquad (15)$$

$$h_{t,j} = \left(\sum_{i=1}^{n}(w_{t,ij}x_{t,i}) + b_{k,j}\right); \quad \begin{cases} i = 1,2,...,n \\ j = 1,2,...,m \end{cases}, \qquad (16)$$

$$r_{t,j} = f_{hidden}\left(h_{t,j}\right) = f\left(\sum_{i=1}^{n}w_{t,ij}x_{t,i} + b_{k,j}\right), \qquad (17)$$

so, the output signal can be calculated as

$$y_t = f_{output}\left(\sum_{j=1}^{m}(w_{t,j}r_{t,j}) + b_y\right); \quad j = 1,2,...,m, \qquad (18)$$

where, $x_{t,i}$ is input, $h_{t,j,}$ and $r_{t,j}$ is input and output of the hidden layer, $b_{k,j}$ and b_y are the bias factor (i.e., for the ith node of the hidden layer) and the bias factor of the neuron in the output layer, respectively, $w_{t,ij}$ and $w_{t,i}$ are connection weights, and y_t is output. The schematic diagram of elucidated multi-layer feedforward NNs can be illustrated in Fig. 3. The structure of implemented NN has one hidden layer, whose sigmoid activation function is presented by

$$r_{t,j} = \frac{1}{1 + e^{-h_{t,j}}}, \qquad (19)$$

or can also be generalized as

$$r_{t,j} = \begin{cases} 1 & h_{t,j} \ge 0 \\ 0 & h_{t,j} < 0 \end{cases}. \qquad (20)$$

Before proceeding, it is better to mention that proper data selection is the most important point in the system. In real systems, training data should be big data like days, months, or
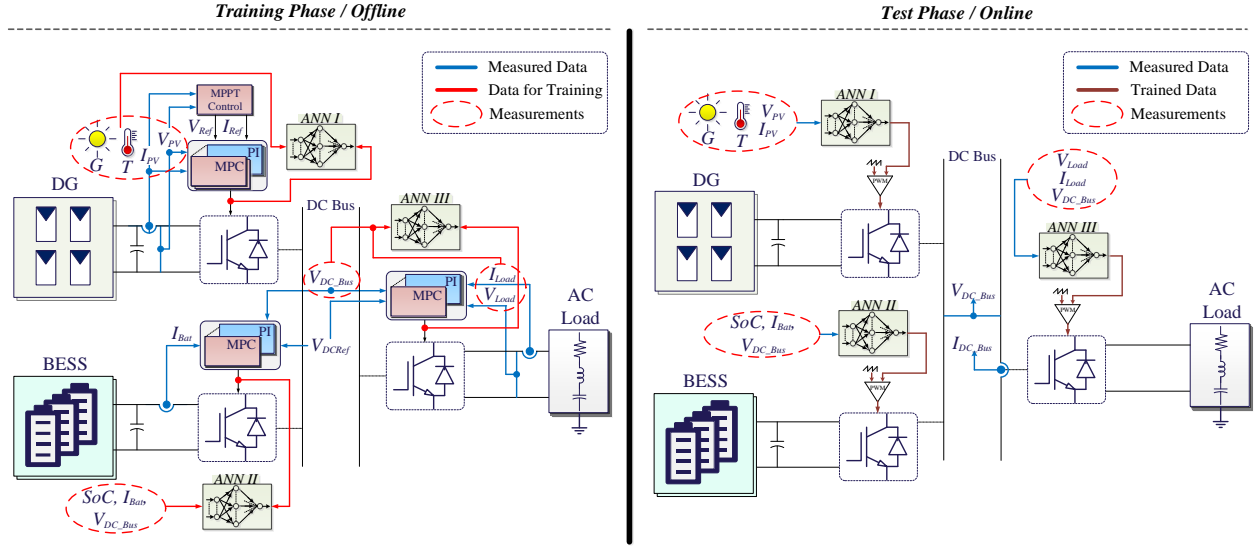
Fig. 4. Operation overview of PV-Battery-based DC microgrid with MPC and conventional-PI controllers at discrete times for training and exploitation phases.
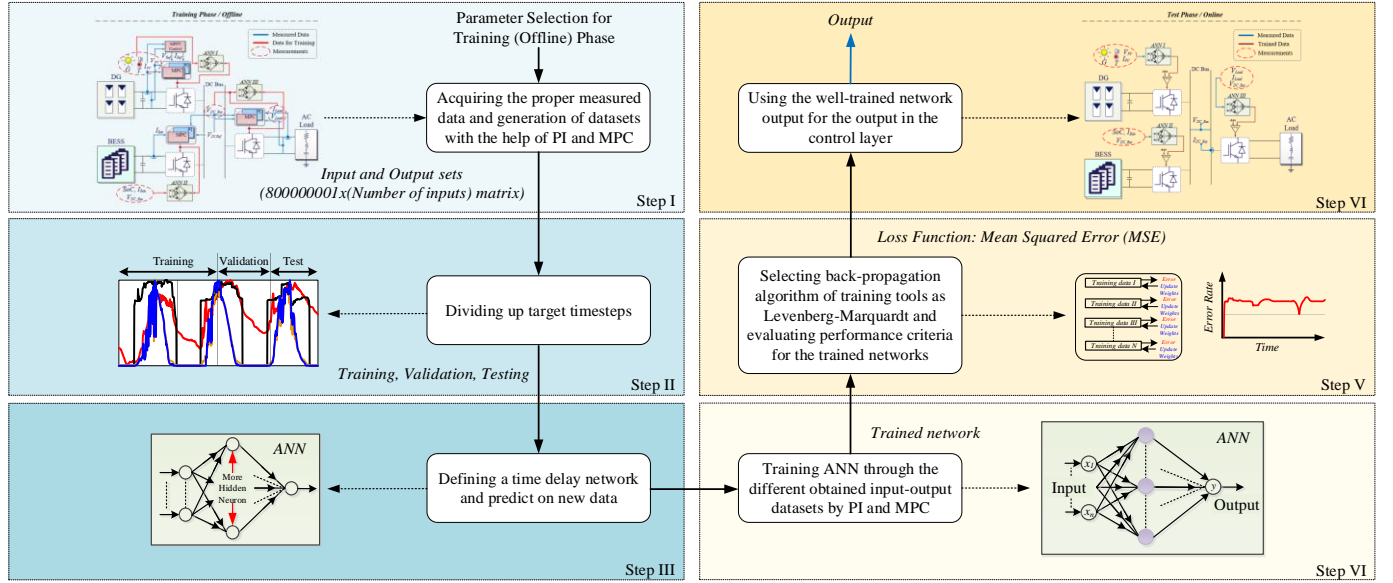

Fig. 5. Application steps of deployment of ANN-based proposed system.

longer to train the system properly according to the application type. Here, we have measured datasets, and thus we have embedded the scaled data into the simulation. For our study, one simulation period is enough for gathering the desired training data. The gathered data can be utilized to create input and output data sets, and based on which the optimized values of the W_t, B_k, and b_y can be obtained. After calculating the weight and bias factors, the well-tuned ANNs can be implemented in the system. Upon considering the performance criteria in (21) and (22) of the trained ANNs, to obtain high accuracy, the correlation coefficient (R) should reflect convergence to 1 (one), and mean squared error (MSE) should be near 0 (zero) as possible as much.

$$R = \frac{1}{m} \sum_{t=1}^{m} \left(\frac{y_{ref}(t) - \mu_{y_{ref}}}{\sigma_{y_{ref}}} * \frac{y(t) - \mu_y}{\sigma_y} \right), \quad (21)$$

$$MSE = \sqrt{\frac{1}{m} \sum_{t=1}^{m} (y_{ref}(t) - y(t))^2}, \quad (22)$$

where, $y_{ref}(t)$ is the desired value, $y(t)$ is the estimated value of the proposed method, and also μ and σ are the mean and standard deviation of the values, respectively. To begin with, the outputs of the ANNs that belong to a static nonlinear relationship with inputs are chosen with the aim of estimating the data for the power converters. Then, suitable inputs to be chosen for outputs are specified. While the system operates in the training phase, the inputs and outputs of ANNs are gathered to be trained by being measured variables such as relevant meteorological, current, and voltage data. Obtaining satisfactory results from the trained ANNs is related to selection proper data, convenient ANN parameters, diversifying training data with enough sample time. After getting desirable training results, the prior controllers are deactivated, and the outputs of the ANNs are linked to the controllers in the exploitation phase. Supposing

that the ANN results look reasonable, it is better to include this ANN into the system permanently after validating its performance with different inputs and outputs obtained for the training. The backpropagation algorithm is performed to initiate the process, including inputs in the input layer, 10 hidden neurons in the hidden layer, and output in the output layers. The target classes are divided for training, validation, and testing parts, selected as 70%, 15%, and 15%, respectively, at 1000 epochs. Due to being selected simulation sample time (Ts) as 5e-9 sec and simulation period (ΔT) as 4 sec, the number of elements can be calculated regarding $(1/Ts)*(\Delta T)$. So, it is notable to mention that the measured training datasets from the measurement devices have been embedded into the simulation as an 800000001x(*Number of inputs*) matrix, representing dynamic data 800000001-1 time steps of input elements and targeted 800001x1(i.e., *Number of output* is equal to 1) matrix as output, representing dynamic output data 800000001-1 time steps of one element.

Firstly, the same input datasets have been utilized for PI-trained ANNs. Then PI-trained ANNs have been implemented in the test (online) phase and obtained the results as can be seen in Fig. 4. Secondly, after obtaining the data from measurements through the MPC in the training (offline) phase, the ANNs are trained well and ready for applying in the test i.e., exploitation (online) phase. The online phase corresponds to working with the proposed ANN-based control technique. In other words, the data are gathered preliminarily, trained for ANNs in the offline phase, then started up working through ANNs without any previous controllers. The trained ANNs provide the duty cycles for PWM signals to the power converters rapidly without any computation effort.

The application steps of deployment of ANN-based proposed control scheme can be mainly aligned with six steps including proper datasets generation with PI and MPC techniques and defining the paradigms (*Step I*), dividing up the target timesteps (*Step II*), selecting training tools as a back-propagation algorithm (*Step III*), training process (*Step IV*), evaluating the performance criteria with the least *MSE* value (*Step V*), and implementation into the system with exploitation phase (*Step VI*). After completing these all steps in Fig. 5, the scheme is ready to implement the well-trained ANN as the last stage. As shown in Table II, inputs and outputs of used ANN on the relevant controllers and their best performance validation values are given. N is the number of ANN that gives duty cycles (d_N) as output for PWM signals to be connected to the power converters' switches. The duty cycle ratio is estimated with the ANN structure by considering the maximum duty cycle constraints. After providing a reliable duty cycle ratio, then the PWM signals are produced by the PWM generator to drive the converter. It is important to point out that networks are not only trained under normal operating conditions but also variable input characteristics. Thereby, well-trained ANNs desired error rates provide the control reliability of the system.

IV. SIMULATION RESULTS

For the first application, it is considered to be that the main controller of the system has been adopted as a cascaded-PI

TABLE II
INPUTS AND OUTPUTS OF ANNs' ELEMENTS ON RELEVANT CONTROLLER

USED SPACE	ANN-ELEMENTS			
	TARGET CONTROL	INPUT	OUTPUT	BEST VALIDATION PERFORMANCE OF *MSE*
ANN I	PV Converter	G, T, V_{PV}, I_{PV}	d_I	2.0232e-6 (PI) 2.9324e-6 (MPC)
ANN II	BESS Converter	I_{Bat}, SoC, V_{DC_Bus}	d_{II}	7.3112e-5 (PI) 9.6784e-5 (MPC)
ANN III	Load Inverter	V_{Load}, I_{Load}, V_{DC_Bus}	d_{III}	4.9614e-4 (PI) 1.6784e-4 (MPC)

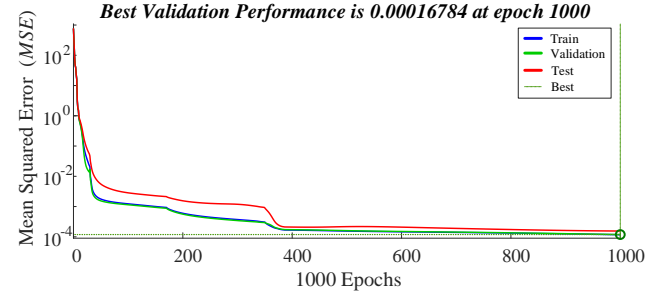Fig. 6. *MSE* value for d_{III} output during the training until 1000 epoch size.

TABLE III
PARAMETERS OF AC LOAD COMPONENTS

AC LOADS	POWERS	OPERATION-TIME
Load I	440 W	0.40 s - 0.98s & 3.5s - 3.95s
Load II	260 W	1.02 s - 1.93 s
Load III	350 W	1.99 s - 3.00 s
Load IV	160 W	2.15 s - 2.91 s
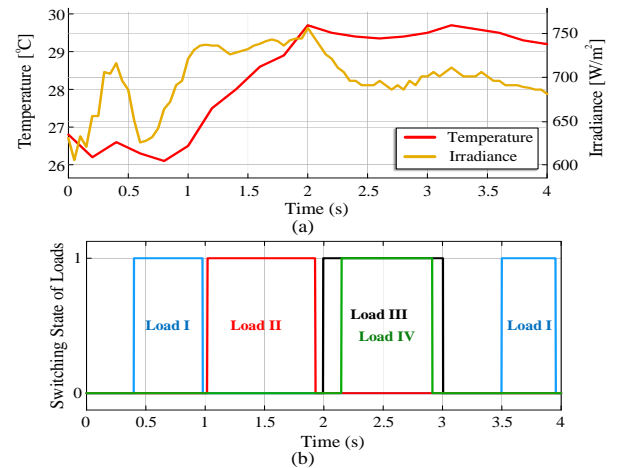
Fig. 7. Variable inputs and outputs: (a) Temperature and solar irradiance, and (b) switching state (event) of loads.

reference voltage-current controller. Likewise, in [45], rapid changes can be controlled effectively using the same cascaded-PI controller for PV-Battery-based applications. As proposed in [46], the evidence we have comprehended some advantages to prefer a cascaded-PI voltage-current controller for a hybrid wind-solar-battery-based microgrid. DGs' further optimal operations effectively provide the DC microgrids' resilient response, implementing cascaded-PI for BESS's primary control. To compare our promising results obtained through the applied controllers, we found it appropriate to perform

Fig. 8. Experimental setups in the laboratory; (a) BESS, on the roof of faculty building: (b) Weather station for meteorological data, and (c) PV-based DG.
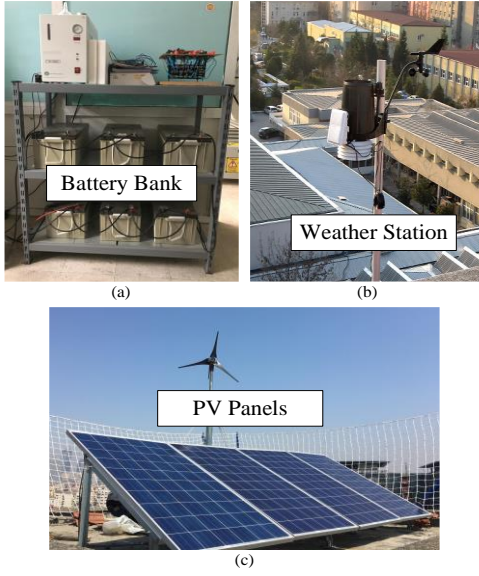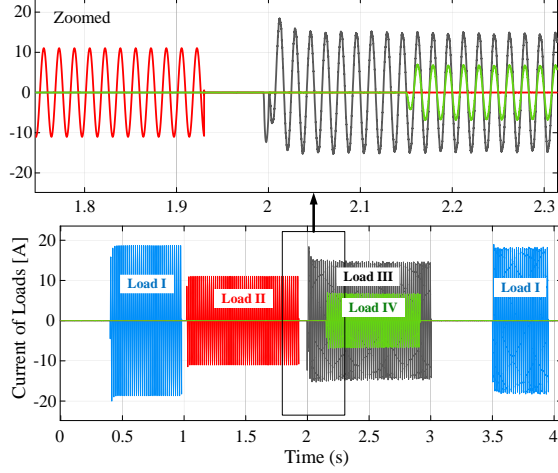

Fig. 9. Currents of load shedding during operation.

TABLE IV

THE COMPARISON OF APPLIED CONTROLLERS FOR DC-BUS VOLTAGE

FEATURES	CONTROLLERS			
	CASCADED-PI	MPC	ANN-BASED PI	ANN-BASED MPC
Slew Rate-V_{90-10}/T_R	Slow 5.84 V/ms	Slower 3.62 V/ms	Fastest 2.61 V/ms	Fast 3.05 V/ms
Voltage Oscilla.-ΔV	High 3.01V	Average 1.90 V	Less 1.51 V	Least 1.15 V
Comp. Burden	Average	High	Lowest	Low
Response Time-T_{RES}	13.23 ms	14.12 ms	5.99 ms	6.60 ms
Robustness	Worse	Average	Good	Better

cascaded-PI and then MPC on the system as a solid basis. The simulation studies have been done in the MATLAB/Simulink software environment. The system has been simulated under variable input like irradiance, temperature, and variable output, i.e., considering different load conditions that do operate distinct operation-times. Due to the natural structure of ANNs, it is inevitable that the results of the training obtained with the
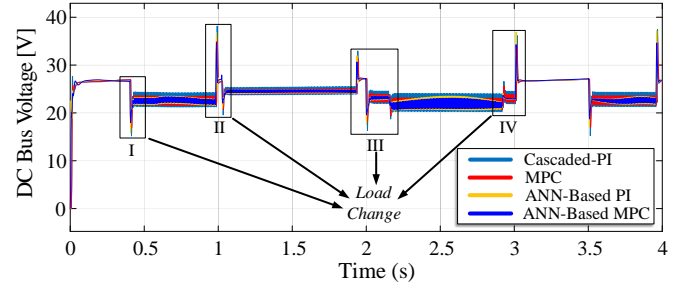
Fig. 10. Variation of DC bus voltage under input and output (load) change.
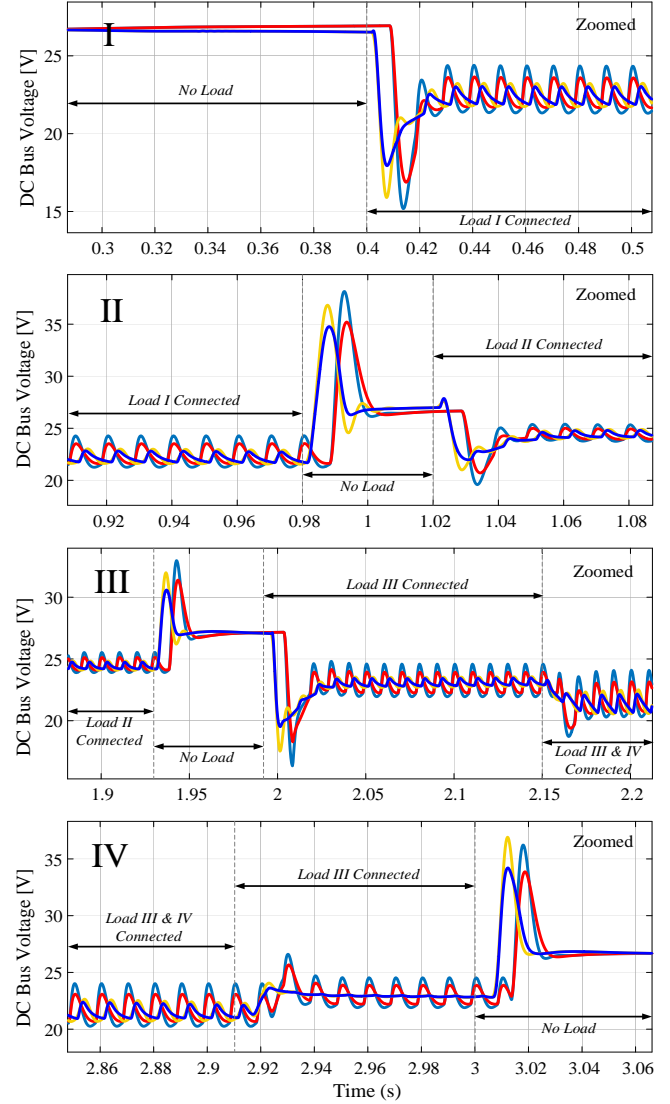
Fig. 11. Zoomed DC bus voltage under input and output (load) change.

same data sets and the same structural configurations will be different. During testing of the proposed method, the results of more than one training process with the same datasets were compared to each other, and the error results obtained with MPC-based training always outperformed lower performance than those obtained with PI-based training. Thus, we have included the best *MSE* result couples obtained as a result of the pieces of training in Table II. With a theoretical perspective, the best validation performance is evaluated by the best validation performance of *MSE* value as validation target timestamps are used to measure network generalization and to halt the training

Fig. 12. Variation of DC bus current under load change condition.

Fig. 13. Zoomed DC bus current under input and output (load) change.

process when generalization stops improving with the validation check. Fig. 6 shows one of the best validation performance of *MSE* results during the training process.

Our model setup bears a close resemblance to the real system; thus, we have preferred to use AC loads and grid parts with its own EMS. In particular, the results have been analyzed and compared with each other in terms of steady and dynamic pe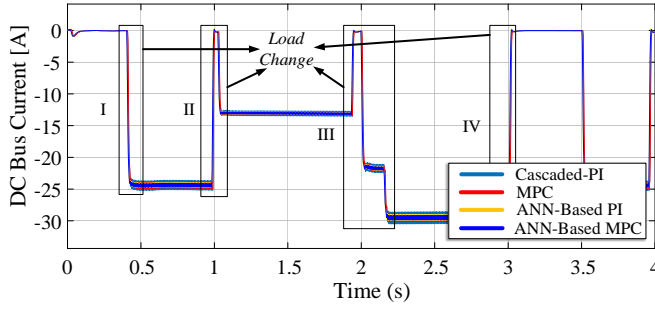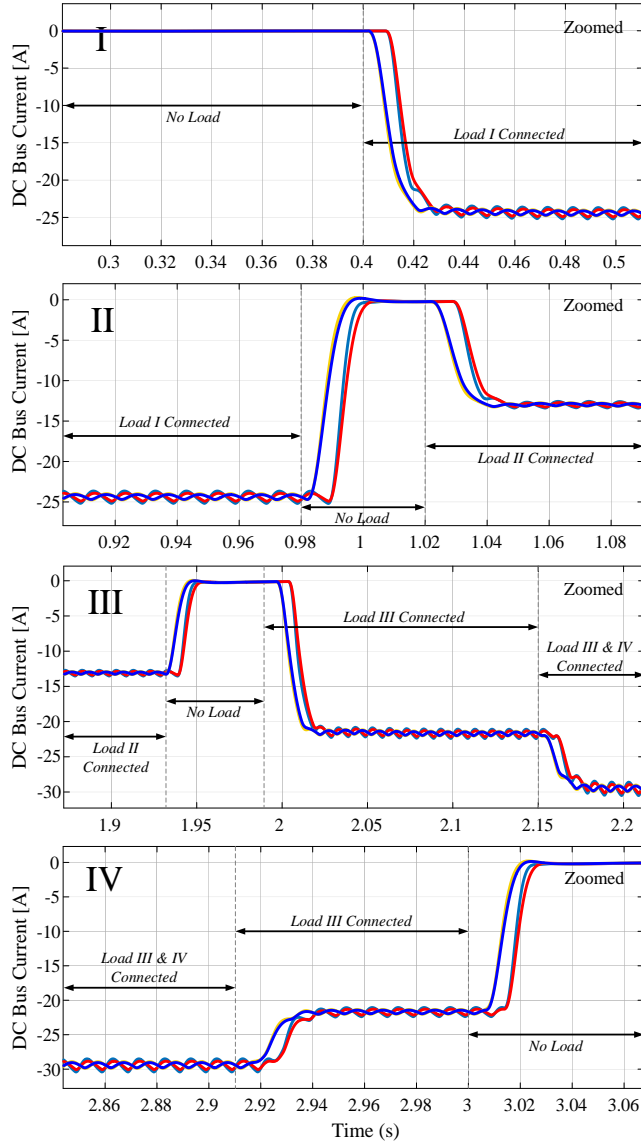rformance. Table III expresses the loads' rating power and their run-time during simulation to evaluate the system's behavior. As can be extracted from Table III, the loads' rating

power is expressed, and the loads are involved in the system at different and same times.

The PV side has two main inputs as temperature and solar irradiance. These variables can be shown in Fig. 7 (a), which give rise to unstable behavior regarding inputs and outputs (loads). At a definite time-interval, Load III and IV are connected. Then, Load I is reconnected in the same sequence, as shown in Fig. 7 (b). To reach realistic results, inputs have been measured and utilized through a weather station, as shown in Fig. 8 (b). Furthermore, the simulation results have been obtained through a strong model of the real system, as seen in Fig. 8 (a) and (c), measured, analyzed, and resembled its behavior. As seen in Fig. 9, the loads are fed smoothly.

For distinguishing between results, the MPC and then MPC-aided ANN was implemented in addition to conventional cascaded-PI controllers. Furthermore, the DC bus is supposed to be assessed in detail due to being the system's backbone. Therefore, we have focalized the DC bus variables such as voltage and current stress to prove the proposed method's effectiveness in balancing input and output changes. To this end, the DC bus voltage alteration, i.e., V_{DC_Bus} can be expressed in Fig. 10 for all controllers. Some critical points of the load change were zoomed in to visualize for better illustration. The characteristic of the DC bus voltages for various time intervals can be investigated in Fig. 11. On the other hand, the DC bus current variation comes from the BESS converter (I_{Bat}) to the inverter, i.e., I_{DC_Bus} can be examined in Fig. 12 with its zoomed ones in Fig. 13.

V. DISCUSSION AND FUTURE WORK

As anticipated, our results prove that the MPC-aided ANN carries out the system properly under unstable input and output conditions. For better illustration of the results for each controller can be aligned as:

i. The coefficients of the cascaded-PI controller [21], [45], [46] can be adjusted faster, although the system can show unstable behavior with large gains of the PI;

ii. PI-trained ANN controller has superior performance for achieving more stable oscillation when compared to conventional-PI;

iii. Unlike this unstable situation, the MPC can alleviate voltage stress to a certain extent in DC bus without any other methods; nevertheless, the MPC suffers from the computational effort, make the system somewhat slow;

iv. To eliminate this issue, MPC-trained ANN seems a good and straightforward choice for compensating the stress with its desired features in Table IV. Also, ANNs could be improved by optimized for each iteration.

Additionally, the training datasets have been generated with the help of related controllers, i.e., PI-trained ANNs have been trained through the data that is obtained with the PI controller, and the MPC one has been implemented likewise. As a result, it is distinct that ANN-based PI shows inferior performance compared to the ANN-based MPC due to being trained in the dataset which has been formed through the conventional-PI controller. So far, the results have been encouraging; therefore, one promising application of our technique would be implementing this approach with both controllers in a real-time system. It is worth mentioning that the loads' character is critical

This article has been accepted for publication in a future issue of this journal, but has not been fully edited. Content may change prior to final publication. Citation information: DOI 10.1109/TEC.2021.3118664, IEEE Transactions on Energy Conversion

10

for comprehending the system's general behavior. Before proceeding to future work as a control application of experimental setup instead of only simulating, we have mentioned control of the PV-based DG, BESS, and real AC loads models that we have, in fact, within the scope of the laboratory.

VI. CONCLUSION

This paper investigated and compared the concept and phenomena of different control applications in PV-Battery-based DC microgrid for stabilization. The results were obtained for comparing each performance under variable climate conditions. The results show different performances related to the training data quality that is arisen from the controller. A comprehensive comparison of the results proved clearly in terms of more robustness, faster dynamics, lower oscillation, and better steady-state performance, which also corresponds to the desired transient response, high flexibility, less computational effort, and better error tolerance, and no needed global information. The variation of V_{DC_Bus} and I_{DC_Bus} under variable input-output conditions such as different power generations and load conditions in the proposed method possesses superior performance over the other three by all means among tried methods. Since the obtained results exhibit the proposed control strategy's efficacy to lessen the instability issues and achieve effective attenuation of oscillations, these results have further strengthened our confidence in the ANN method, which is affiliated with strong control techniques.

VII. ACKNOWLEDGMENT

REFERENCES

[1] Y. Shan, J. Hu, K. W. Chan, Q. Fu, and J. M. Guerrero, "Model Predictive Control of Bidirectional DC-DC Converters and AC/DC Interlinking Converters-A New Control Method for PV-Wind-Battery Microgrids," *IEEE Trans. Sustain. Energy*, vol. 10, no. 4, pp. 1823–1833, 2019.

[2] N. Bayati, H. R. Baghaee, A. Hajizadeh, and M. Soltani, "Localized Protection of Radial DC Microgrids With High Penetration of Constant Power Loads," *IEEE Syst. J.*, pp. 1–12, 2020.

[3] W. Su, S. Yu, H. Li, H. Iu, and T. Fernando, "An MPC-based Dual-solver Optimization Method for DC Microgrids with Simultaneous Consideration of Operation Cost and Power Loss," *IEEE Trans. Power Syst.*, pp. 1–11, 2020.

[4] W. W. A. G. Silva, T. R. Oliveira, and P. F. Donoso-Garcia, "An improved voltage-shifting strategy to attain concomitant accurate power sharing and voltage restoration in droop-controlled dc microgrids," *IEEE Trans. Power Electron.*, vol. 36, no. 2, pp. 2396–2406, 2021.

[5] M. Nasir, S. Iqbal, and H. A. Khan, "Optimal Planning and Design of Low-Voltage Low-Power Solar DC Microgrids," *IEEE Trans. Power Syst.*, vol. 33, no. 3, pp. 919–2928, 2018.

[6] X. Wu *et al.*, "A Two-Layer Distributed Cooperative Control Method for Islanded Networked Microgrid Systems," *IEEE Trans. Smart Grid*, vol. 11, no. 2, pp. 942–957, 2020.

[7] F. Li, Z. Lin, Z. Qian, J. Wu, and W. Jiang, "A dual-window DC bus interacting method for DC microgrids hierarchical control scheme," *IEEE Trans. Sustain. Energy*, vol. 11, no. 2, pp. 652–661, 2020.

[8] N. Jin, S. Hu, C. Gan, and Z. Ling, "Finite States Model Predictive Control for Fault-Tolerant Operation of a Three-Phase Bidirectional AC/DC Converter under Unbalanced Grid Voltages," *IEEE Trans. Ind. Electron.*, vol. 65, no. 1, pp. 819–829, 2018.

[9] H. U. R. Habib, S. Wang, M. R. Elkadeem, and M. F. Elmorshedy, "Design Optimization and Model Predictive Control of a Standalone Hybrid Renewable Energy System: A Case Study on a Small Residential Load in Pakistan," *IEEE Access*, vol. 7, pp. 117369–117390, 2019.

[10] S. R. Mohapatra and V. Agarwal, "An advanced voltage support scheme considering the impact of zero-sequence voltage under microgrid faults using model predictive control," *IEEE Trans. Ind. Electron.*, vol. 67, no. 10, pp. 8957–8968, 2020.

[11] Y. Shan, J. Hu, Z. Li, and J. M. Guerrero, "A Model Predictive Control for Renewable Energy Based AC Microgrids Without Any PID Regulators," *IEEE Trans. Power Electron.*, vol. 33, no. 11, pp. 9122–9126, 2018.

[12] Z. Karami, Q. Shafiee, Y. Khayat, M. Yaribeygi, T. Dragicevic, and H. Bevrani, "Decentralized Model Predictive Control of DC Microgrids with Constant Power Load," *IEEE J. Emerg. Sel. Top. Power Electron.*, pp. 1–10, 2019.

[13] M. M. Mardani, M. H. Khooban, A. Masoudian, and T. Dragicevic, "Model Predictive Control of DC-DC Converters to Mitigate the Effects of Pulsed Power Loads in Naval DC Microgrids," *IEEE Trans. Ind. Electron.*, vol. 66, no. 7, pp. 5676–5685, 2019.

[14] Q. Xiao, L. Chen, H. Jia, P. W. Wheeler, and T. Dragicevic, "Model Predictive Control for Dual Active Bridge in Naval DC Microgrids Supplying Pulsed Power Loads Featuring Fast Transition and Online Transformer Current Minimization," *IEEE Trans. Ind. Electron.*, vol. 67, no. 6, pp. 5197–5203, 2020.

[15] L. Chen *et al.*, "Predictive Control Based DC Microgrid Stabilization with the Dual Active Bridge Converter," *IEEE Trans. Ind. Electron.*, vol. 67, no. 10, pp. 8944–8956, 2020.

[16] T. Dragičević, "Dynamic Stabilization of DC Microgrids with Predictive Control of Point-of-Load Converters," *IEEE Trans. Power Electron.*, vol. 33, no. 12, pp. 10872–10884, 2018.

[17] Q. Xu, Y. Yan, C. Zhang, T. Dragicevic, and F. Blaabjerg, "An Offset-Free Composite Model Predictive Control Strategy for DC/DC Buck Converter Feeding Constant Power Loads," *IEEE Trans. Power Electron.*, vol. 35, no. 5, pp. 5331–5342, 2020.

[18] E. Kowsari, J. Zarei, R. Razavi-Far, M. Saif, T. Dragicevic, and M. H. Khooban, "A Novel Stochastic Predictive Stabilizer for DC Microgrids Feeding CPLs," *IEEE J. Emerg. Sel. Top. Power Electron.*, 2020.

[19] M. B. Shadmand, R. S. Balog, and H. Abu-Rub, "Model predictive control of PV sources in a smart DC distribution system: Maximum power point tracking and droop control," *IEEE Trans. Energy Convers.*, vol. 29, no. 4, pp. 913–921, 2014.

[20] X. Zhang, B. Wang, U. Manandhar, H. Beng Gooi, and G. Foo, "A Model Predictive Current Controlled Bidirectional Three-Level DC/DC Converter for Hybrid Energy Storage System in DC Microgrids," *IEEE Trans. Power Electron.*, vol. 34, no. 5, pp. 4025–4030, 2019.

[21] C. Wang, J. Duan, B. Fan, Q. Yang and W. Liu, "Decentralized High-Performance Control of DC Microgrids," *IEEE Trans. Smart Grid*, vol. 10, no. 3, pp. 3355-3363, 2019.

[22] Y. Yang, S. C. Tan, and S. Y. R. Hui, "Mitigating distribution power loss of dc microgrids with DC electric springs," *IEEE Trans. Smart Grid*, vol. 9, no. 6, pp. 5897–5906, 2018.

[23] S. R. Mohapatra and V. Agarwal, "Model Predictive Controller With Reduced Complexity for Grid-Tied Multilevel Inverters," *IEEE Trans. Ind. Electron.*, vol. 66, no. 11, pp. 8851-8855, 2019.

[24] T. Dragičević and M. Novak, "Weighting Factor Design in Model Predictive Control of Power Electronic Converters: An Artificial Neural Network Approach," *IEEE Trans. Ind. Electron.*, vol. 66, no. 11, pp. 8870-8880, 2019.

[25] S. Wang, T. Dragicevic, Y. Gao, and R. Teodorescu, "Neural Network based Model Predictive Controllers for Modular Multilevel Converters," *IEEE Trans. Energy Convers.*, doi: 10.1109/TEC.2020.3021022.

[26] I. S. Mohamed, S. Rovetta, T. D. Do, T. Dragicević, and A. A. Z. Diab, "A Neural-Network-Based Model Predictive Control of Three-Phase Inverter With an Output *LC* Filter," *IEEE Access*, vol. 7, pp. 124737-124749, 2019.

[27] J. Duan, Z. Yi, D. Shi, C. Lin, X. Lu, and Z. Wang, "Reinforcement-Learning-Based Optimal Control of Hybrid Energy Storage Systems in Hybrid AC–DC Microgrids," *IEEE Trans. Ind. Informat.*, vol. 15, no. 9, pp. 5355-5364, Sept. 2019.

[28] M. A. Khan, A. Haque, V. S. B. Kurukuru, and M. Saad, "Advanced Control Strategy with Voltage Sag Classification for Single-Phase Grid-Connected Photovoltaic System," *IEEE Trans. Emerg. Sel. Topics Ind. Electron.*, doi: 10.1109/JESTIE.2020.3041704.

This article has been accepted for publication in a future issue of this journal, but has not been fully edited. Content may change prior to final publication. Citation information: DOI 10.1109/TEC.2021.3118664, IEEE Transactions on Energy Conversion

11

[29] A. Rosato, M. Panella, R. Araneo, and A. Andreotti, "A Neural Network Based Prediction System of Distributed Generation for the Management of Microgrids," *IEEE Trans. Ind. Appl.*, vol. 55, no. 6, pp. 7092-7102, 2019.

[30] N. Chettibi, A. Mellit, G. Sulligoi, and A. Massi Pavan, "Adaptive Neural Network-Based Control of a Hybrid AC/DC Microgrid," *IEEE Trans. Smart Grid*, vol. 9, no. 3, pp. 1667-1679, 2018.

[31] Z. Farooq, T. Zaman, M. A. Khan, Nasimullah, S. M. Muyeen, and A. Ibeas, "Artificial Neural Network Based Adaptive Control of Single Phase Dual Active Bridge With Finite Time Disturbance Compensation," *IEEE Access*, vol. 7, pp. 112229-112239, 2019.

[32] A. N. Akpolat, M. R. Habibi, E. Dursun, A. E. Kuzucuoglu, Y. Yang, T. Dragicevic, and F. Blaabjerg, ``Sensorless control of DC microgrid based on artifcial intelligence," *IEEE Trans. Energy Convers.*, vol. 36, no. 3, pp. 2319-2329, 2021.

[33] M. Ahmed, A. Vahidnia, M. Datta, and L. Meegahapola, "An Adaptive Power Oscillation Damping Controller for a Hybrid AC/DC Microgrid," *IEEE Access*, vol. 8, pp. 69482-69495, 2020.

[34] A. N. Akpolat, E. Dursun and A. E. Kuzucuoglu, "Deep Learning-Aided Sensorless Control Approach for PV Converters in DC Nanogrids," *IEEE Access*, vol. 9, pp. 57949-57966, 2021.

[35] X. Liu, H. Jiang, Y. Wang, and H. He, "A Distributed Iterative Learning Framework for DC Microgrids: Current Sharing and Voltage Regulation," *IEEE Trans. Emerg. Topics Comput. Intell.*, vol. 4, no. 2, pp. 119-129, 2020.

[36] W. Dong, S. Li, X. Fu, Z. Li, M. Fairbank and Y. Gao, "Control of a Buck DC/DC Converter Using Approximate Dynamic Programming and Artificial Neural Networks," *IEEE Trans. Circuits Systs. I: Regular Papers,* vol. 68, no. 4, pp. 1760-1768, 2021.

[37] B. Adineh, M. R. Habibi, A. N. Akpolat, and F. Blaabjerg, "Sensorless Voltage Estimation for Total Harmonic Distortion Calculation using Artificial Neural Networks in Microgrids," *IEEE Trans. Circuits Systs. II: Express Briefs*, vol. 68, no. 7, pp. 2583- 2587, 2021.

[38] L. Xu, R. Cheng, and J. Yang, "A New MPPT Technique for Fast and Efficient Tracking under Fast Varying Solar Irradiation and Load Resistance," *Int. J. Photoenergy*, pp. 1–18, 2020.

[39] A. N. Akpolat, Y. Yang, F. Blaabjerg, E. Dursun and A. E. Kuzucuoglu, "Design Implementation and Operation of an Education Laboratory-Scale Microgrid," *IEEE Access,* vol. 9, pp. 57949-57966, 2021.

[40] T. Dragicevic, "Model Predictive Control of Power Converters for Robust and Fast Operation of AC Microgrids," *IEEE Trans. Power Electron.*, vol. 33, no. 7, pp. 6304–6317, 2018.

[41] M. R. Z. Sabegh and C. Bingham, "Model predictive control with binary quadratic programming for the scheduled operation of domestic refrigerators," *Energies*, vol. 12, p. 4649, 2019.

[42] E. F. Camacho and C. Bordons, "Model predictive control," in *Advanced Textbooks in Control and Signal Processing*, London, UK, 2007.

[43] M. Inc., "MATLAB MPC Toolbox," *Mathwork Inc.*, 2020. https://se.mathworks.com/products/mpc.html.

[44] A. N. Akpolat, E. Dursun, and A. E. Kuzucuoglu, ``AI-aided control of a power converter in wind energy conversion system,'' in *Proc. Innov. Intell. Syst. Appl. Conf. (ASYU)*, Oct. 2020, pp. 1–6.

[45] N. Saxena, I. Hussain, B. Singh, and A. L. Vyas, "Implementation of a Grid-Integrated PV-Battery System for Residential and Electrical Vehicle Applications," *IEEE Trans. Ind. Electron.*, vol. 65, no. 8, pp. 6592–6601, 2018.

[46] J. P. C. Silveira, et al., "Power management of energy storage system with modified interlinking converters topology in hybrid AC/DC microgrid," *Int. J. Electr. Power Energy Syst.,* vol. 130, pp. 106880, 2021.

Alper Nabi Akpolat (S'19–M'21) received the B.Sc. degree in Electrical-Electronics Engineering and the M.Sc. degree in Mechatronics Engineering from Firat University, Elazig, Turkey, in 2012 and 2015, respectively. He is currently working toward the Ph.D. degree in Electrical-Electronics Engineering and also serving as a Research Assistant, from Faculty of Technology, at Marmara University, Istanbul, Turkey.

From March 2019, he has been a Guest Ph.D. student during one year with Department of Energy Technology, Aalborg University, Denmark as part of YÖK-YUDAB scholarship. His current research interests include renewable energy systems, PV systems, DC microgrids, control of distributed generation systems, neural networks, and applied artificial intelligence in power electronics and power systems.

Mohammad Reza Habibi (S'19) was born in Tehran, Iran. He is currently working toward the Ph.D. degree with the Department of Energy Technology, Aalborg University, Denmark. He was also a Visiting Research Scholar with the Department of Electrical Power Engineering and Mechatronics, Tallinn University of Technology, Tallinn, Estonia.

His current research interests include intelligent energy systems, application of artificial intelligence in power electronics and power systems, advanced control of power converters, modeling and control of energy storage systems, modeling and secure control of DC distribution systems and microgrids, and cyber-physical systems.

Hamid Reza Baghaee (S'08–M'17) was born in Kashan, Iran, in June 1984 and received his Ph.D. degree in Electrical Engineering from Amirkabir University Technology (AUT) in 2017. From 2007 to 2017, he was a teaching and research assistant in the department of electrical engineering of AUT. He is the author of two books, three published book chapters, 80 ISI-ranked journal papers (mostly in IEEE, IET, and Elsevier journals), 55 conference papers, and the owner of a registered patent. He has many HOT and HIGHLY-CITED papers among his journal papers, based on SciVal and Web of Science statistics. His special fields of interest are micro and smart grids, cyber-physical systems, application of power electronics in power systems, distributed generation and renewable energy resources, FACTS CUSTOM Power devices, and HVDC systems, power system operation and control, real-time simulation of power systems, microgrids, and power electronic converters, and application of artificial intelligence in power systems.

Dr. Baghaee is also the winner of four national and international prizes, as the best dissertation award, from the Iranian scientific organization of smart grids (ISOSG) in December 2017, Iranian energy association (IEA) in February 2018, AUT in December 2018, and IEEE Iran Section in May 2019 for his Ph.D. dissertation. In August 2019, he joined AUT as an associate research professor in the department of electrical engineering. He is the project coordinator of the AUT Pilot Microgrid Project as one of the sub-projects of the Iran Grand (National) Smart Grid Project. He has been a co-supervisor of more than Ph.D. and M.Sc. students since 2017. He was a short-term scientist with CERN and ABB, Switzerland. He was selected as the top 1% reviewer of engineering in September 2018 and the top 1% reviewer of engineering and cross-field in September 2019. Dr. Baghaee is a member and secretary chair at the IEEE Iran Section communication committee and member of IEEE, IEEE Smart Grid Community, IEEE Internet of Things Technical Community, IEEE Big Data Community, and IEEE Sensors Council. Since August 2021, he has been elected as the Member of the Board and Chairman of the Committee on Publications and Conferences at the Iran Scientific Organization of Smart Grids (ISOSG). He is also the reviewer of several IEEE and IET journals and guest editor of several special issues in IEEE, IET, Elsevier, MDPI, and scientific program committees of several IEEE conferences. From December 2020, he has served as an associate editor of the IET Journal of engineering. He has also been selected as the best and outstanding review of several journals such as IEEE Transactions on Power System (Top 0.66% of reviewers, in 2020), Elsevier Control Engineering Practice (in 2018, 2019, and 2020), and Wiley International Transaction on Electrical Energy Systems in 2020, and the Pablon best reviewer in Engineering (in 2018), and both engineering and cross-field (in 2019). He has been selected as the Star Reviewer of IEEE JESTPE and IEEE Power Electronics Society in 2020, commemorated, and presented during the IEEE ECCE 2021 conference, 10-14 October in Vancouver, Canada.

This article has been accepted for publication in a future issue of this journal, but has not been fully edited. Content may change prior to final publication. Citation information: DOI 10.1109/TEC.2021.3118664, IEEE Transactions on Energy Conversion

12

Erkan Dursun (S'05–M'13) received the B.Sc., M.Sc., and Ph.D. degrees in Electric Education from the Faculty of Technical Education, Marmara University, Istanbul, Turkey, in 2001, 2006, and 2013, respectively. From 2010 to 2012, he was a Visiting Fellow with the United Nations Industrial Development Organization–International Centre for Hydrogen Energy Technologies (UNIDO-ICHET).

From 2012 to 2013, he was a Researcher with the Joint Research Center, European Commission, Italy. He is currently an Assistant Professor with the Department of Electrical and Electronics Engineering, Faculty of Technology, Marmara University, Istanbul, Turkey. His research interests include Distributed Generation, Hybrid Power Systems, and Smart Grid.

Ahmet Emin Kuzucuoğlu (M'99) is an Associate Professor at Marmara University, Turkey. He received his B.Sc. degree from Electronics and Telecommunication Engineering Department, Istanbul Technical University, Turkey, in 1985 and he received his M.Sc. and Ph.D. degrees from Marmara University, in 1994 and 2000, respectively.

He has been in England and the United States of America in 1987 as part of YÖK-World Bank Vocational School Project. He has been in Lithuania in July-2006 as part of EU Leonardo da Vinci Type A mobility project. He is an Associate Professor with the Department of Electrical-Electronics Engineering. His current research interests include industrial automation, robotics, AI, control theory and applications.

Yongheng Yang (SM'17) received the B.Eng. degree in Electrical Engineering and Automation from Northwestern Polytechnical University, China, in 2009 and the Ph.D. degree in Energy Technology (power electronics and drives) from Aalborg University, Denmark, in 2014.

He was a postgraduate student with Southeast University, China, from 2009 to 2011. In 2013, he spent three months as a Visiting Scholar at Texas A&M University, USA. Since 2014, he has been with the Department of Energy Technology, Aalborg University, where he became a tenured Associate Professor in 2018. In January 2021, he joined Zhejiang University, China, where he is currently a ZJU100 Professor with the Institute of Power Electronics, College of Electrical Engineering. His current research interests include the grid-integration of photovoltaic systems and control of power converters, in particular, the mechanism and control of grid-forming power converters and systems.

Dr. Yang was the Chair of the IEEE Denmark Section (2019-2020). He is an Associate Editor for several IEEE Transactions/Journals. He is a Deputy Editor of the *IET Renewable Power Generation* for Solar Photovoltaic Systems. He was the recipient of the 2018 *IET Renewable Power Generation* Premium Award and was an Outstanding Reviewer for the IEEE TRANSACTIONS ON POWER ELECTRONICS in 2018. He received the 2021 Richard M. Bass Outstanding Young Power Electronics Engineer Award from the IEEE Power Electronics Society (PELS). In addition, he has received two IEEE Best Paper Awards. He is currently the Secretary of the IEEE PELS Technical Committee on Sustainable Energy Systems.

Tomislav Dragičević (S'09–M'13–SM'17) received the M.Sc. and the industrial Ph.D. degrees in Electrical Engineering from the Faculty of Electrical Engineering, University of Zagreb, Croatia, in 2009 and 2013, respectively. From 2013 until 2016 he has been a Postdoctoral researcher at Aalborg University, Denmark. From 2016 until 2020 he was an Associate Professor at Aalborg University, Denmark. Currently, he is a Professor at the Technical University of Denmark.

He made a guest professor stay at Nottingham University, UK during spring/summer of 2018. His research interest is application of advanced control, optimization and artificial intelligence inspired techniques to provide innovative and effective solutions to emerging challenges in design, control and diagnostics of power electronics intensive electrical distributions systems and microgrids. He has authored and co-authored more than 330 technical publications (more than 150 of them are published in international journals, mostly in IEEE), 10 book chapters and a book in this field, as well as filed for several patents.

He serves as an Associate Editor in the IEEE TRANSACTIONS ON INDUSTRIAL ELECTRONICS, in IEEE TRANSACTIONS ON POWER ELECTRONICS, in IEEE EMERGING AND SELECTED TOPICS IN POWER ELECTRONICS and in IEEE INDUSTRIAL ELECTRONICS MAGAZINE. Prof. Dragičević is a recipient of the Končar prize for the best industrial PhD thesis in Croatia, a Robert Mayer Energy Conservation award, and he is a winner of an Alexander von Humboldt fellowship for experienced researchers.

Frede Blaabjerg (S'86–M'88–SM'97–F'03) was with ABB-Scandia, Randers, Denmark, from 1987 to 1988. From 1988 to 1992, he got the PhD degree in Electrical Engineering at Aalborg University in 1995. He became an Assistant Professor in 1992, an Associate Professor in 1996, and a Full Professor of power electronics and drives in 1998. From 2017 he became a Villum Investigator. He is honoris causa at University Politehnica Timisoara (UPT), Romania and Tallinn Technical University (TTU) in Estonia.

His current research interests include power electronics and its applications such as in wind turbines, PV systems, reliability, harmonics and adjustable speed drives. He has published more than 600 journal papers in the fields of power electronics and its applications. He is the co-author of four monographs and editor of ten books in power electronics and its applications.

He has received 33 IEEE Prize Paper Awards, the IEEE PELS Distinguished Service Award in 2009, the EPE-PEMC Council Award in 2010, the IEEE William E. Newell Power Electronics Award 2014, the Villum Kann Rasmussen Research Award 2014, the Global Energy Prize in 2019 and the 2020 IEEE Edison Medal. He was the Editor-in-Chief of the IEEE TRANSACTIONS ON POWER ELECTRONICS from 2006 to 2012. He has been Distinguished Lecturer for the IEEE Power Electronics Society from 2005 to 2007 and for the IEEE Industry Applications Society from 2010 to 2011 as well as 2017 to 2018. In 2019-2020 he served as a President of IEEE Power Electronics Society. He has been Vice-President of the Danish Academy of Technical Sciences.

He is nominated in 2014-2020 by Thomson Reuters to be between the most 250 cited researchers in Engineering in the world.